THE ASTROPHYSICAL JOURNAL, 296:774–783, 1985 September 15


# VACUUM ULTRAVIOLET STUDIES OF ELECTRON IMPACT OF HELIUM: EXCITATION OF He $n\,{}^1P^o$ RYDBERG SERIES AND IONIZATION-EXCITATION OF $He^+$ $nl$ RYDBERG SERIES

D. E. SHEMANSKY,[1] J. M. AJELLO,[2] D. T. HALL,[1] AND B. FRANKLIN[2]

*Received 1984 December 18; accepted 1985 March 25*


## ABSTRACT

Laboratory measurements of the electron excitation cross sections of emission in the He Rydberg series ($1s^2\ {}^1S$–$1snp\ {}^1P^o$) for $n = 2, 3, 4$ have been obtained. The cross sections were estimated by two methods: (1) analysis of calibrated laboratory spectra placed on an absolute scale using the H Ly$\alpha$ dissociative excitation standard and (2) analysis of relative cross section data using a modified Born approximation. A new method has been developed for the application of the Bethe-Born approximation using experimental relative excitation functions that does not require extrapolation in a Fano plot in the determination of the absolute cross section. The two methods agree to within 3% for the 58.4 nm line when allowance is made for cascade transitions. We find the direct excitation cross sections at 200 eV for the $n = 2, 3, 4$ members of the $1s$–$np$ Rydberg series to be $(7.94 \pm 1.75) \times 10^{-18}$, $(2.06 \pm 0.45) \times 10^{-18}$ and $(0.87 \pm 0.19) \times 10^{-18}$ cm$^2$, respectively. There results agree well within experimental uncertainty with Born method results. Ionization-excitation cross sections of He have been measured for emission in the He II $2l$–$4l$ 121.51 nm and $2l$–$3l$ 164.0 nm transitions. It appears that published electron impact experimental measurements of the two-electron process of ionization-excitation impact are generally in agreement, especially on the energy dependence of excitation functions, but show significant differences with theoretical calculations.


*Subject headings:* laboratory spectra — transition probabilities — ultraviolet: spectra

## I. INTRODUCTION

There have been many measurements of the electron impact cross sections of the first three members of the helium Rydberg series ($1s^2\ {}^1S^o$–$1snp\ {}^1P^o$). These cross sections were placed on an absolute scale by the well-known Bethe-Born approximation based on optical oscillator strengths (Westerveld, Heideman, and Van Eck 1979, hereafter WHE); Donaldson, Hender, and McConkey 1972, hereafter DHM; Van Eck and de Jongh 1970; Moustafa Moussa, de Heer, and Schutten 1969). Up to this time there has been no absolute measurement of the cross sections based on an optical calibration as a test of the validity of the Bethe-Born approximation, nor has there been a published calibrated extreme ultraviolet (EUV) fluorescence emission spectrum (50–60 nm) of this series. The present work also includes measurements of ionization-excitation functions of He and the far-ultraviolet (FUV) fluorescence spectrum of the He II $2l$–$nl$ series.

The polarization free excitation function of He I emission multiplets from threshold to 2 keV has been accurately measured by others (WHE; DHM). We therefore study and model the VUV emission spectrum of He at one energy, 200 eV, on the basis of an optical calibration technique in a crossed-beam system (Ajello *et al.* 1984). In this work a calibrated spectrum of the He Rydberg series is obtained in the 50–60 nm region measured at 54°.7, the "magic angle," and corrected for polarization effects. The absolute cross section in the present experimental method is derived from the H Ly$\alpha$ dissociative excitation cross section (Shemansky, Ajello, and Hall 1985, hereafter Paper I). It is then of considerable interest to compare the He I cross section determined in this way with the absolute cross section derived from the relative excitation function and the application of the Born approximation directly to the He I transition. The latter method generally obtains the cross section through extrapolation in a Fano plot (see DHM). We have examined this technique of obtaining the absolute cross section, and propose a new method, mentioned above, which eliminates the need for extrapolation through a process of fitting an analytic function to the experimental excitation function. The method in addition has the advantage of providing information on the physics of the excitation process, for example, of the contribution of exchange reactions. We find, as discussed below, that the absolute cross sections of the He I transitions obtained in relation to the H Ly$\alpha$ atomic hydrogen cross section and through the modified Born approximation are in excellent agreement, provided that we apply the new H Ly$\alpha$ dissociative excitation cross section (Paper I) in obtaining the result.

Simultaneous ionization-excitation of He leads to a far-ultraviolet (FUV) spectrum with emissions at 121.51 and 164.04 nm, the Balmer $\alpha$ and $\beta$ transitions of He II. The measurements in this case are obtained at a beam angle of 90°. These two He II cross sections, from branching-ratio considerations allow one to establish the He II EUV cross section for the L$\beta$ and L$\gamma$ transitions of He II in the 20–30 nm region. Ionization-excitation of He is of fundamental theoretical importance, since it is the simplest two-electron excitation process. We find that most of the experimental data, including the present work, are in good agreement with respect to the shape of the excitation functions of the He II emissions, and uniformly in basic disagreement with theoretical calculations. There is some disagreement among experimental estimates of absolute cross sections, but the differences are not considered to be serious.

Helium is the second most abundant element. Electron collisional excitation and ionization of helium is an important process in the heating of the interstellar gas (Shull 1979). The production of UV photons requires accurate cross sections for

[1] Lunar and Planetary Laboratory, University of Arizona, Tucson.
[2] Jet Propulsion Laboratory, California Institute of Technology, Pasadena.

modeling purposes. He II (164.0 nm) emission is observed in the outer atmospheres of cool stars (Ayres *et al.* 1983).

This paper is one of a series of VUV emission studies of gases by electron impact of planetary, cometary, and astrophysical interest by our laboratory. Previous work has been published on $H_2$ (Ajello, Srivastava, and Yung 1982; Ajello *et al.* 1984; Shemansky and Ajello 1983), $H_2O$ (Ajello 1984), $O_2$ (Ajello and Franklin 1985), $N_2$ (Ajello and Shemansky 1985), $CS_2$ (Ajello and Srivastava 1981).

## II. EXPERIMENTAL

The experimental apparatus and VUV calibration technique have been described in detail in earlier publications (Ajello and Srivastava 1981; Ajello *et al.* 1984). In brief, the instrument consists of an electron impact emission chamber in tandem with a UV spectrometer. A magnetically collimated beam of electrons is crossed with a beam of gas formed by a capillary array. The inelastic electron-particle collisions produced can be observed at any angle with respect to the electron beam axis.

As a preliminary study the electron beam axis was rotated with respect to the optic axis, and the observed intensities were found to be weakly dependent on this angle at 200 eV because of polarization of the radiation as shown experimentally and theoretically by Mumma *et al.* (1974). A single measurement of the intensity at the "magic angle" allows determinations of the total radiation field of the atom. However, the radiation field of the He atom observed at the magic angle is polarized, and the optical system is calibrated for unpolarized light described below. It can be shown (J. W. McConkey 1984, private communication) after the methods of Heddle and Keesing (1968) and Clout and Heddle (1969) that the intensity ratio at the detector between a polarized beam of light of intensity $I(P)$ and an unpolarized beam of light of intensity $I(0)$ is

$$\frac{I(P)}{I(0)} = \frac{\{1 + [2(1 - P)/(1 + P)]K_{\perp}/K_{\parallel}\}}{1 + 2(K_{\perp}/K_{\parallel})}, \qquad (1)$$

where $P$ is polarization and $K_{\perp}$ and $K_{\parallel}$ are the instrument sensitivities for light polarized perpendicular and parallel, respectively, to the monochromator entrance slit. The polarization fraction from the He 58.4 nm source at 200 eV is 12.8% (Mumma *et al.* 1974, Table 2). The ratio $K_{\perp}/K_{\parallel}$ at 58.4 nm for an osmium grating with a 32° angle of incidence is 0.585 (Ajello *et al.* 1984). Thus we find

$$I(0) = I(P) \times 1.13 .$$

The He 58.4 nm signal measured at the magic angle was multiplied by 1.13 to correct the source for polarization.

On the other hand, the angular dependence of the H Lyα radiation field produced by dissociative excitation is weak. At 200 eV the polarization of H Lyα is found to be about 4% (Malcolm, Dassen, and McConkey 1979) and leads to an insignificant difference (~1%) between apparent cross section and excitation cross section. Thus we can safely assume that the radiation field of Lyα at 200 eV is unpolarized.

The relative wavelength sensitivity of the optical system of the monochromator and channeltron detector for unpolarized light was described previously (Ajello *et al.* 1984). The same calibration curves given in this reference apply to the data measured here. The relative accuracy of the calibration from 50 to 121.6 nm is estimated to be 15%.

The background gas pressure for the determination of cross sections is maintained below $2 \times 10^{-6}$ torr. This pressure results in optical depths at the line center of He I 58.4 nm of less than 0.2 for the 16 cm optical path length. Below this pressure the He I 58.4 nm cross section is found to be independent of pressure as illustrated in Figure 1.

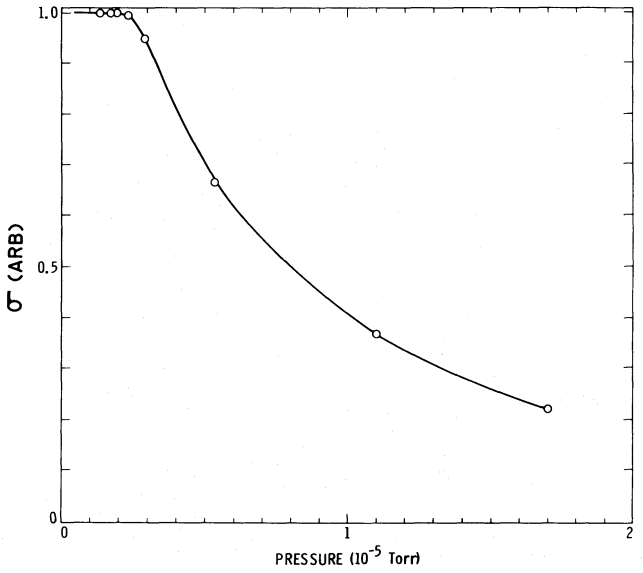


FIG. 1.—Linearity test for cross section vs. background gas pressure in the chamber for the He I 58.43 nm emission feature.

The absolute calibration of the optical system relies on the H Lyα dissociative excitation cross section of $H_2$ at 200 eV, which we determined in Paper I to have the value of $5.87 \times 10^{-18}$ cm$^2$. The estimated uncertainty of this value is 15%.

### *a*) He I 58.4 nm *Cross Section*

The absolute cross section of the He I 58.4 nm transition is determined by the relative flow technique developed at the Jet Propulsion Laboratory (Srivastava, Chutjian, and Trajmar 1975; Trajmar and Register 1984). In this method the H Lyα emission signal from $H_2$, the standard gas, is compared with the signal from He I 58.4 nm over a range of background gas pressures from $1 \times 10^{-6}$ to $2 \times 10^{-5}$ torr as shown in Figure 1. A direct comparison of the two gases can be made in the region where the signal is linear with pressure (less than $2 \times 10^{-6}$ torr as shown in Fig. 1 for He). These signal intensities are divided by pressure and electron beam current in order to be proportional to the apparent cross section. The H Lyα photon signal has been corrected for the background contribution by molecular $H_2$ bands as described in Paper I. This critical calibration was also performed at the magic angle. The result shows that the direct excitation cross section of He I 58.43 nm at 200 eV is $7.94 \times 10^{-18}$ cm$^2$. The uncertainty is the root sum square 1 $\sigma$ uncertainty of the following: (1) 15% uncertainty in our published Lyα cross section, (2) 15% uncertainty in relative wavelength calibration, and (3) 5% uncertainty in signal statistics and repeatability. This cross section can be compared with the value ($7.75 \times 10^{-18}$ cm$^2$) obtained from the modified Born approximation and the DHM–WHE excitation functions.

### *b*) He I 50–60nm *Cross Sections*

We show in Figure 2 the calibrated emission spectrum of He + *e* (200 eV) at a resolution of 0.5 nm for a 57?4 emission

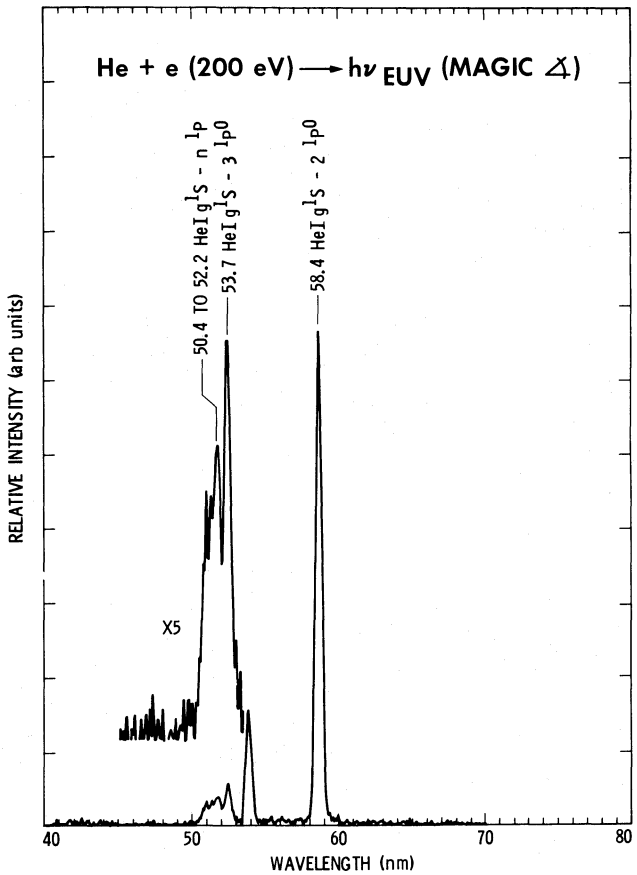


FIG. 2.—Calibrated laboratory spectrum of He at 200 eV at "magic angle," 54°.8. Beam experiment performed at a background chamber pressure of $2.5 \times 10^{-6}$ torr. He beam density is $2 \times 10^{12}$ cm$^{-3}$; electron beam current, $\sim 200$ $\mu$A.

angle. The relative intensities of the *np* Rydberg series members are independent of beam intercept angle. Clearly identifiable peaks are found up to principal quantum number $n = 7$, though not resolved for $n \geq 5$. A comparison of our cross section results at 200 eV with previous results is shown for the first three Rydberg series members and for the sum of $n \geq 5$ Rydberg series members in Table 1. We have corrected our measured emission cross section for the small amount of cascade from $^1S$ and $^1D$ into the $n\ ^1P$ state, to obtain an estimated direct excitation cross section which is then suitable for comparison with the Bethe approximation and with the modified Born approximation results described below. We suggest that the modified Born approximation results lead to a more accurate evaluation of the absolute cross section than the Fano plot extrapolation technique, although both are sensitive to data quality. The cascade correction (DHM; WHE) is given in Table 1, column (11), and is always less than 6% of the total measured cross section. This component is important only at low energy ($E \leq 50$ eV) where forbidden excitation to the upper state of the cascade source is most probable. We include an integrated cross section for $n \geq 5$ for the whole Rydberg series in Table 1.

The absolute cross sections based on the Bethe approximation obtained through application of Fano plots (Table 1, cols. [4]–[8]) and the results here (col. [3]) agree within the experimental error (6%–24%). However, the agreement between the modified Born approximation (col. [10]), and the optical calibration data (1%–12%, col. [3]) is improved because of a small reduction of the cross sections in the present analysis relative to the original work of DHM and WHE (col. [4]). Since the $n = 2, 3, 4, \ldots$ levels are close in excitation energy (21.22, 23.09, 23.74, ... eV), the relative dependence of the cross section on principal quantum number is expected to be nearly equal to the relative dependence of the optical oscillator strengths (col. [9]; Wiese, Smith, and Glennon 1966). The present measurements of the $n = 4$ and $n \geq 5$ Rydberg series represent the most accurate measurement to date of these cross sections, because of the increasing difficulty of obtaining the polarization constant $C_{ij}$, in the Bethe approximation for $n \geq 4$ (DHM). We find the total cross section for direct excitation of the $np\ ^1P$ series to be $1.20 \times 10^{-17}$ cm$^2$ at 200 eV.

In conclusion, it appears that the modified Born formulation using optical oscillator strengths to normalize high-energy laboratory cross sections ($E > 1$ keV) of helium results in improved agreement with the present optically calibrated measurements for $n \leq 3$ at 200 eV. In this regard the quoted uncertainties in the optical oscillator strengths are 1% for $n = 2$, 3% for $n = 3$, and 10% for $n \geq 4$ (Wiese, Smith, and Glennon 1966). Thus, for high Rydberg members with $n \geq 4$, an evaluation of a high-resolution spectrum from a calibrated optical system is the preferred method of cross section determination.

### c) He II *UV Cross Sections*

In addition to the He I ($1s\ ^1S$–$np\ ^1P^o$) Rydberg series, we have studied the H$\alpha$ and H$\beta$ transitions of He II at 164.04 and 121.51 nm, respectively. The FUV spectrum is shown in Figure 3 in order to provide an indication of signal and noise levels. The estimated cross sections at 200 eV are given in Table 2. These transitions originate from the $4l$ and $3l$ excited states as shown in the transition diagram in Figure 4, where $l = s, p$, and $d$. Other measurements of these transitions have been obtained by Moustafa Moussa and de Heer (1967) and are shown in Table 2. The experimental work of the latter reference also includes estimates of the cross sections of the 25.63 nm $1s$–$3p$ and 468.6 nm $3l$–$4l$ transitions (Table 2). The VUV measurements described by Moustafa Moussa and de Heer were placed on an absolute scale by comparison with the $e + H_2$ CUV (countable ultraviolet) excitation cross section as measured by Fite and Brackmann (1958). The most accurate value produced by Moustafa Moussa and de Heer is presumably that for the 121.5 nm transition, because instrument relative sensitivity as a function of wavelength was not well established. On this basis the cross sections for the 164.04 nm $2l$–$3l$ and 121.51 nm $2l$–$4l$ transitions obtained in the present work and those of Moustafa Moussa and de Heer are considered to be in good agreement. The transitions with the same upper principal quantum number have cross sections in a fixed relationship, determined by the relative population rates of the orbitals within the state.

In detail, the $1s$–$3p$ cross section for the 25.63 nm multiplet is given by

$$\sigma_{3p1s} = \sigma_{3l2l} \frac{A_{3p1s}}{A_{3p}} \left( R_{sp3} \frac{A_{3s2p}}{A_{3s}} + \frac{A_{3p2s}}{A_{3p}} + R_{dp3} \frac{A_{3d2p}}{A_{3d}} \right)^{-1}, \quad (2)$$

where $R_{sp3} = \sigma_{3s}/\sigma_{3p}$ and $R_{dp3} = \sigma_{3d}/\sigma_{3p}$. The emission cross section for the transition array (near-energy degeneracy for the $L = S, P, D$ multiplets) or individual multiplets depending on

1985ApJ...296..774S

TABLE 1

RELATIVE AND ABSOLUTE DIRECT EXCITATION CROSS SECTIONS OF HELIUM AT 200 eV[a]

| Multiplet (1) | $\lambda$ (nm) (2) | This Work[b] (3) | DHM[c] (4) | WHE[d] (5) | Moustafa Moussa, de Heer, and Schutten (1969)[d] (6) | Kim and Inokuti (1968)[d] (7) | Van Eck and de Jongh (1970)[d] (8) | Born Limit[e] (9) | Modified Born Approximation[f] (10) | Cascade[g] (11) |
|---|---|---|---|---|---|---|---|---|---|---|
| $2\,^1P^o$: | | | | | | | | | | |
| Relative | 58.43 | 1.00 | 1.00 | 1.00 | 1.00 | 1.00 | 1.00 | 1.00 | 1.00 | ... |
| Absolute | ... | 7.94 | 8.2 | 8.3 | 6.6 | 9.4 | 8.6 | ... | 7.75 | 0.4 |
| $3\,^1P^o$: | | | | | | | | | | |
| Relative | 53.70 | 0.26 | 0.29 | 0.25 | 0.28 | 0.25 | 0.25 | 0.27 | 0.23 | ... |
| Absolute | ... | 2.05 | 2.4 | 2.1 | 2.0 | 2.3 | 2.1 | ... | 1.81 | 0.07 |
| $4\,^1P^o$: | | | | | | | | | | |
| Relative | 52.22 | 0.11 | 0.11 | ... | 0.10 | 0.10 | 0.10 | 0.11 | 0.11 | ... |
| Absolute | ... | 0.87 | 0.88 | ... | 0.72 | 0.93 | 0.89 | ... | 0.86 | ~0.02[h] |
| $n \geq 5\,^1P^o$: | | | | | | | | | | |
| Relative | <51.56 | 0.15 | ... | ... | ... | ... | ... | 0.15 | ... | ... |
| Absolute | ... | 1.11 | ... | ... | ... | ... | ... | ... | ... | ... |
| Total for $n\,^1P$ Rydberg series | ... | 12.0 | ... | ... | ... | ... | ... | ... | ... | ~0.5 |

[a] Direct excitation, and cascade cross sections in units of $10^{-18}$ cm$^2$. Cascade contribution subtracted as in DHM and WHE.
[b] Emission cross sections converted to direct excitation cross sections. Crossed beam experiment.
[c] Crossed beam experiment; Bethe-Born approximation.
[d] Static experimental system; Bethe-Born approximation.
[e] Oscillator strength ratio from Wiese, Smith, and Glennon 1966. See text.
[f] Analytic approximation using Table 2 coefficients.
[g] From DHM.
[h] Estimated.

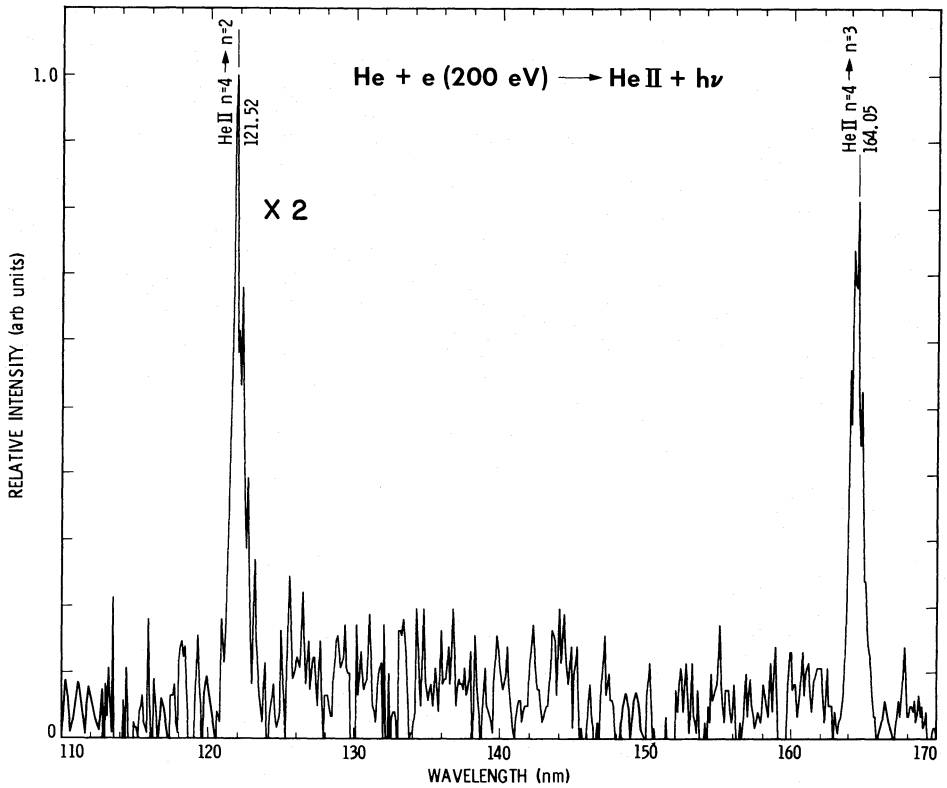


FIG. 3.—Calibrated FUV spectrum of He I at 1.2 nm resolution excited by 200 eV electrons. The spectrum contains the 121.52 and 164.05 nm lines of He II. A background signal of H Lyα produced by electron-excited $H_2O$ has been subtracted from the spectrum.

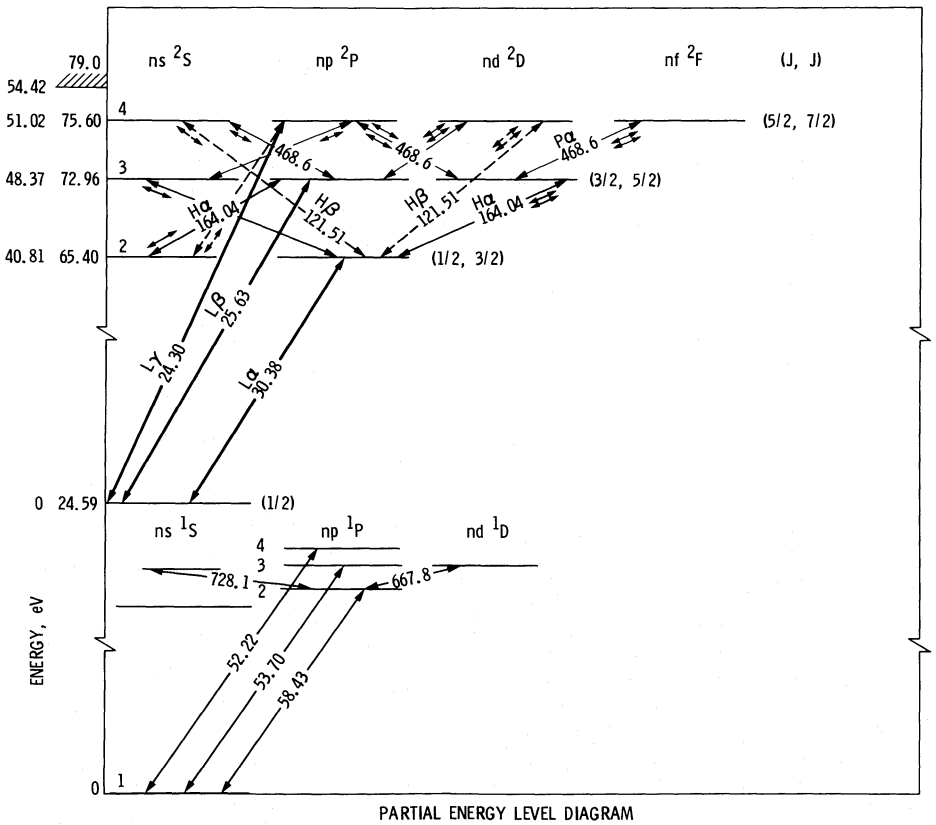


FIG. 4.—Simplified energy level diagram of He I and He II

TABLE 2

A. Cross Sections for Ionization-Excitation of Helium by Electron Impact at 200 eV

| Transition | Wavelength (nm) | $\sigma$ ($10^{-20}$ cm$^2$) | Reference |
|---|---|---|---|
| 1s–2p | 30.38 | 3.7 | Dalgarno and McDowell 1956 |
| | | 56 | Bloemen *et al.* 1981 |
| | | 61 | Forand, Becker, and McConkey 1985 |
| 1s–3p | 25.63 | <33 | from eq. (2); see text |
| | | 0.8 | Dalgarno and McDowell 1956 |
| | | 3.0 | Moustafa Moussa and de Heer 1967 |
| 2–3 | 164.04 | 4.51 | this work |
| | | ~8 | Moustafa Moussa and de Heer 1967; uncalibrated |
| 1s–4p | 24.30 | <16 | from eq. (2); see text |
| | | 0.3 | Dalgarno and McDowell 1956 |
| 2–4 | 121.51 | 2.26 | this work |
| | | 2.7 | Moustafa Moussa and de Heer 1967 |
| 3–4 | 468.6 | 0.42 | St. John and Lin 1964 |
| | | 0.37 | Lee and Lin 1965 |
| | | 0.49 | Moustafa Moussa and de Heer 1967 |
| | | 1.60–0.77 | from eq. (3); see text |

B. Recommended Cross Sections at 200 eV and Corresponding Coefficients[a] for Analytic Excitation Functions

| Transition | Wavelength (nm) | $E$ (rydbergs) | $C_5$ | $\sigma$ ($10^{-20}$ cm$^2$) |
|---|---|---|---|---|
| 1s[b] | ... | 1.807 | −3.419 | 3240 |
| 1s–2p[c] | 30.38 | 4.806 | 1.43 − 1[d] | 59 |
| 1s–3p[c] | 25.63 | 5.362 | 6.66 − 3 | 2.5[e] |
| 2l–3l[c] | 164.04 | 5.362 | 1.20 − 2 | 4.5 |
| 1s–4p[c] | 24.30 | 5.557 | 5.25 − 3 | 1.9[e] |
| 2l–4l[c] | 121.50 | 5.557 | 6.35 − 3 | 2.3[e] |
| 3l–4l[c] | 468.6 | 5.557 | 3.86 − 3 | 1.44[e] |
| Σ2l[c] | ... | 4.806 | 3.39 − 1 | 140 |
| Σ3l[c] | ... | 5.362 | 1.89 − 2 | 7.1[e] |
| Σ4l[c] | ... | 5.557 | 1.57 − 2 | 5.7[e] |

[a] See text, eq. (9).
[b] $C_0/C_5 = 5.24 - 3$; $C_7/C_5 = -1.173$; $C_n = 0.0$ for $n = 1, \ldots, 4$.
[c] $C_1/C_5 = -1.1416 - 1$; $C_2/C_5 = 2.2466$; $C_3/C_5 = -7.1203$; $C_4/C_5 = 4.3156$; $C_0 = 0.0$; $C_7 = 0.0$; $\alpha = 0.3850$.
[d] The notation 1.43 − 1 means $1.43 \times 10^{-1}$.
[e] $R_{spm} = 1.44$; $R_{dpn} = 0.1$.

subscript is denoted by $\sigma$, and similarly $A$ denotes the transition probability for the multiplet to the lower state or to all lower states depending on subscript.

A similar equation is obtained for $\sigma_{4p1s}$, the cross section for the 24.3 nm transition, by substituting the subscript 4 for 3 in equation (2). The 2*l*–4*l* and 3*l*–4*l* transitions at 121.51 nm and 468.6 nm originate from the same upper state, and if relative cross sections are known for the $n = 4$ levels, we can evaluate the ratio

$$\sigma_{4l2l}/\sigma_{4l3l} = \left(R_{sp4}\frac{A_{4s2p}}{A_{4s}} + \frac{A_{4p2s}}{A_{4p}} + R_{dp4}\frac{A_{4d2p}}{A_{4d}}\right) \times \left(R_{sp4}\frac{A_{4s3p}}{A_{4s}} + \frac{A_{4p3s} + A_{4p3d}}{A_{4p}} + R_{dp4}\frac{A_{4d3p}}{A_{4d}}\right)^{-1}. \quad (3)$$

The transition probabilities are well-known quantities, and any uncertainty in the relative cross sections depends entirely on uncertainty in the ratios $R_{spn}$ and $R_{dpn}$. These quantities are at present not entirely accessible from the experimental data. Lee and Lin (1965) give theoretical calculations for the $n = 4$ levels, but in our view little weight can be placed on these values because of strong differences with the experimental excitation functions. One point of strong disagreement among the experimental measurements is with the $\sigma_{4l2l}/\sigma_{4l3l}$ ratio. The range of values for the $\sigma_{4l3l}$ cross section based on the measured $\sigma_{4l2l}$ cross section (Table 2) is well above the directly measured cross sections given by St. John and Lin (1964) and Moustafa Moussa and de Heer (1967). We recommend that the 3*l*–4*l* cross section be remeasured at low pressures in order to resolve the issue. Dalgarno and McDowell (1956) have calculated the cross sections for the He II 1*s*, *np* ($n = 2$–4), *nd* ($n = 3$, 4) levels, but again there is strong disagreement with the experimental data both in energy dependences and in magnitudes.

The excitation cross section of the 2*l*–3*l* 164.04 nm transition measured in this work is shown in Figure 5. An analytic fit to the cross section is shown as a curve drawn through the data points (Fig. 5). The shape of the collision strength derived from this excitation function is very similar to those of the 3*l*–4*l* 468.6 nm, 2*l*–4*l* 121.51 nm, and 2*l*–3*l* 164.04 nm transitions measured by Moustafa Moussa, de Heer and Schutten (1967). The shapes of the collision strengths for these transitions have

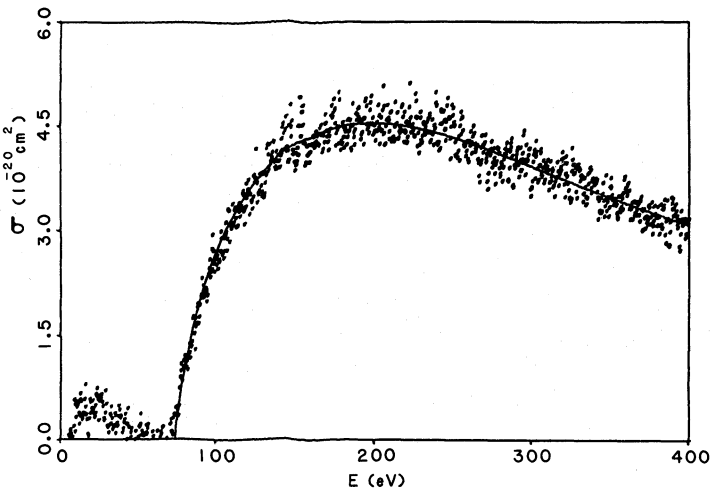


FIG. 5.—Relative excitation function of He II 164.04 nm produced by electron ionization-excitation of He I over the 0–400 eV range measured in a static chamber. The energy width of the electron beam is estimated to be ~1 eV, at a current of 50–100 μA. Chamber pressure is $\sim 10^{-5}$ torr.

an energy dependence that is fundamentally different from that of a Born dipole permitted transition, and is different from the theoretical calculations (Lee and Lin 1965; Dalgarno and McDowell 1956). The collision strengths, plotted in Figure 6, are discussed further in the following section.

### III. A MODIFIED BORN APPROXIMATION

A useful method of establishing absolute cross sections from uncalibrated excitation functions produced in experimental measurements is one of applying the Bethe approximation to the high-energy region of the data, in a Fano plot extrapolation (cf. DHM and Kim and Inokuti 1968). However, it is also a dangerous procedure because the theory applies only to strictly allowed, unmixed transitions. If the transition contained a measurable electron exchange component, for example, the extrapolation process could produce erroneous results caused by subtle departures from linearity in the Fano plot. In the following discussion we propose an alternate method applying a nine-parameter curve-fitting technique that we suggest is superior to a Fano plot because it does not involve extrapolation. The method has an additional advantage, in that it is sensitive to complexities in the transition such as an electron exchange component or configuration mixing.

We suggest that fitting the entire experimental cross section curve from threshold to the maximum available energy is a superior method because it provides measures of the magnitude of the deviation from the Bethe-Born approximation at high energies. The form of the Bethe approximation to the total cross section is more appropriate to ions, in which the cross section acquires a finite value at threshold. Neutral particles, if we neglect polarization effects, have a characteristic zero cross section at threshold. Thus the Bethe formulation

$$\sigma_{ij} = \frac{4\pi a_0^2}{E}\frac{f_{ij}}{E_{ij}} \ln (4C_{ij}E) , \tag{4}$$

where $a_0$ is the Bohr radius, $f_{ij}$ is the absorption oscillator strength, $E_{ij}$ is the transition energy in rydbergs, and $E$ is the electron energy, does not degenerate to zero at threshold unless the constant $C_{ij}$ is given by

$$C_{ij} = \tfrac{1}{4}E_{ij} . \tag{5}$$

If an experimentally derived value of $C_{ij}$ is obtained on the basis of equation (4), as DHM have done, and the value deviates substantially from equation (5), the basic form of the equation will violate the characteristics of the excitation function at some ill-defined minimum energy. The point in energy at which the Bethe-Born approximation completely controls the function becomes a vexing question under these circumstances. The approach that DHM and others take for the derivation of the excitation cross section is based on the properties of equation (4). The equation may be rewritten in the following form:

$$\sigma_{ij}E = 4\pi a_0^2 \frac{f_{ij}}{E_{ij}} (\ln X + \ln 4C_{ij}E_{ij}) . \tag{6}$$

where

$$X = E/E_{ij} . \tag{7}$$

A plot of $\sigma_{ij}E$ versus $\ln X$, if the theory holds, should produce a straight line. In principle, one could then plot experimentally derived relative values of $\sigma_{ij}E$ versus $\ln X$ and obtain an experimental value of $C_{ij}$ at the intercept wherein the extrapolated $\sigma_{ij}E = 0.0$, and thus

$$\ln X' = -\ln (4C_{ij}E_{ij}), \tag{8}$$

where $X'$ is the intercept energy in dimensionless (threshold) units. The practicality of applying this method is limited by how closely the form of equation (4) follows the cross section, and the nature of subtle deviations from the Bethe approximation as one moves from high to low electron energies. The product $\sigma_{ij}E$ is proportional to the collision strength $\Omega_{ij}$, and therefore equation (6) describes a theoretical form for the dependence of the Gaunt factor on energy (see Seaton 1962). However, in general it is a poor approximation to neutral

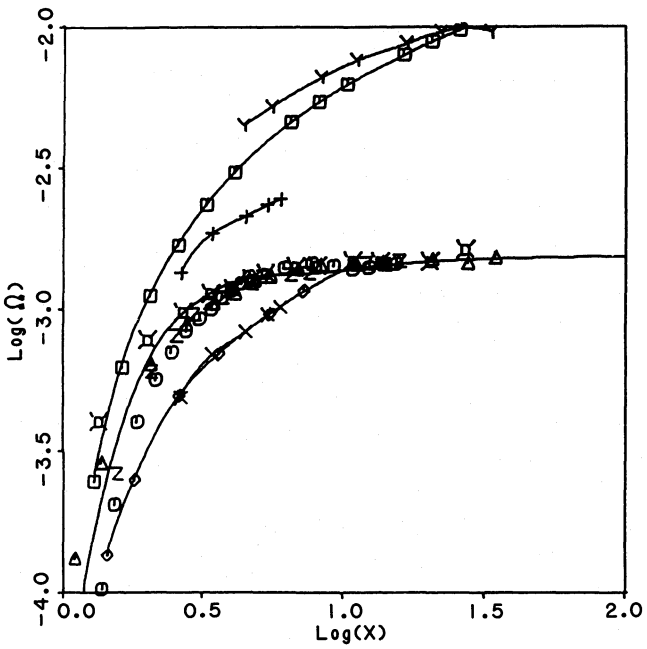


FIG. 6.—Collision strengths for ionization excitation of He into He II ground and excited states as a function of energy in threshold units ($X$). The curves are normalized with arbitrary scale factors. Absolute strengths can be obtained from Table 4. (□) He II 1*s* from Rapp and Golden (see Kieffer and Dunn 1966); (Y) He II 1*s* from Dalgarno and McDowell (1956); (Z) He II 3*l*–4*l* from Moustafa Moussa and de Heer (1967); (⧈) He II 2*l*–4*l* from Moustafa Moussa and de Heer (1967); (△) He II 2*l*–3*l* from Moustafa Moussa and de Heer (1967); (*solid curve*) He II 2*l*–3*l* analytic fit to present measurements; (*crosses*) He II 4*p* from Lee and Lin (1965); (◇) He II 4*p* from Dalgarno and McDowell (1956); (*plus signs*) He II 4*s* from Lee and Lin (1965); (⊙) He II 2*p* from Forand, Becker, and McConkey (1985).

collision-strength characteristics in the threshold region (Seaton 1962), and therefore one runs the risk of producing erroneous cross sections by the method described above. A relation that has been found to produce accurate collision strengths for allowed transitions of a broad range of neutral particle transitions has the following form:

$$\Omega_{ij} = [C_0(1/X^2) + C_5](1 - 1/X) + \sum_{n=1}^{4} C_n(X - 1.0) \exp(-\alpha n X) + C_7 \ln X . \quad (9)$$

where the $C_n$ and $\alpha$ are constants. Equation (9) is a modification of a general form that has been applied to fit analytically numerically calculated and experimental collision strengths for ions (cf. Henry 1981). We note that equation (9) has the basic property of degenerating to a zero value of $\Omega_{ij}$ at threshold ($X = 1.0$), and to the Bethe energy dependence at the high-energy limit:

$$\Omega_{ij} \approx C_5 + C_7 \ln X, \quad X \gg 1 , \quad (10)$$

which is the same form as equation (6). In the Bethe approximation,

$$\Omega_{ij} = \omega_i\left(\frac{8ma_0^2}{\hbar^2}\right)\frac{f_{ij}}{E_{ij}}(\ln X + \ln 4C_{ij}E_{ij}) . \quad (11)$$

where $\omega_i$ is lower state degeneracy, and therefore

$$C_7 = \omega_i\left(\frac{8ma_0^2}{\hbar^2}\right)\left(\frac{f_{ij}}{E_{ij}}\right) = 4.00\left(\frac{f_{ij}}{E_{ij}}\right) \quad \text{for He } {}^1S\text{–}n\ {}^1P , \quad (12)$$

and

$$C_{ij} = (4E_{ij})^{-1} \exp(C_5/C_7) . \quad (13)$$

The constant $C_{ij}$ is related to the angular distribution of the scattered electrons, and enters directly into formulations for the calculation of the energy-dependent polarization of the emitted radiation (McFarlane 1974; Percival and Seaton 1958). Thus the ratio $(C_5/C_7)$ in equation (13) determines the magnitude of the polarization (in the Bethe approximation) of the emitted photons. The remaining constants in equation (9), $C_0$–$C_4$, represent the contributions of electron exchange and configuration mixing to the total collision strength. In the method we apply here the relative values of the constants in equation (9) are fixed in accurately fitting the shape of the excitation function from threshold to the maximum available electron energy. The collision strength can then be placed on an absolute scale by fixing the value of $C_7$ with equation (12). In this case the He I ${}^1S$–2 ${}^1P^o$ cross section is fixed on an absolute scale through equation (12), giving

$$C_7 = 0.7102 .$$

In fitting the absolute cross sections given by DHM and WHE, using equation (9), we obtained values

$$C_7 = 0.744$$

and

$$C_7 = 0.764 .$$

respectively. Thus the DHM and WHE cross sections are 5% and 8% larger than we estimate using the same data.

The present analysis of the data from higher members of the Rydberg series show similar differences, 20% and 15% (${}^1S$–3 ${}^1P$) and 2% (${}^1S$–4 ${}^1P$), with the original DHM and WHE values, consistently below the original cross section estimate. These new cross sections provide improved agreement with the directly measured experimental results obtained for He I in this work at 200 eV as shown in Table 1. Table 3 shows the derived coefficients for equation (9) for the three lower Rydberg levels. Table 4 shows the calculated cross sections using equation (9) compared with the rescaled DHM and WHE cross sections. Agreement of the analytic results with the experimental numbers falls within the stated experimental uncertainties, with the exception of the 3 ${}^1P$ case. The DHM and WHE experiments are not in particularly good agreement in this case, and the analysis reflects the uncertainty. Figure 7 shows plots of the analytic curves against the data in order to illustrate the nature of the deviations. The quality of the results for the He 3 ${}^1P$ state are clearly not comparable to those obtained for the 2 ${}^1P$ and 4 ${}^1P$ states (Fig. 7).

Equation (9) is directly integrable, allowing convenient calculation of rate coefficients. The thermally averaged collision strength $\Omega_{ij}(Y)$ is given by

$$\Omega_{ij}(Y) = C_0\, Y[E_2(Y) - E_3(Y)] \exp(Y) + \sum_{n=1}^{4} C_n\, Y(n\alpha + Y)^{-2} \exp(-n\alpha) + C_5 + [C_7 - C_5\, Y]E_1(Y) \exp(Y) , \quad (14)$$

$$Y = E_{ij}/T_e , \quad (15)$$

TABLE 3

ELECTRON EXCITATION COLLISION STRENGTH COEFFICIENTS FOR THE He ${}^1S$–$n$ ${}^1P^o$ SERIES[a]

| Coefficient | 2 ${}^1P^o$ | 3 ${}^1P^o$ | 4 ${}^1P^o$ |
|---|---|---|---|
| $C_0$ | −0.294283 | −0.716854 − 1 | −0.64430 − 2 |
| $C_1$ | −0.307039 − 1[b] | −0.747927 − 2 | 0.548029 − 2 |
| $C_2$ | 0.1099657 | 0.267869 − 1 | −0.359610 − 1 |
| $C_3$ | −0.491314 − 1 | −0.119681 − 1 | 0.100036 |
| $C_4$ | −0.170969 | −0.359505 − 1 | −0.135187 |
| $C_5$ | −0.312282 | −0.760698 − 1 | −0.536665 − 2 |
| $C_7$ | 0.71020 | 0.17300 | 0.69220 − 1 |
| $\alpha$ | 0.1220 | 0.1470 | 0.160 |
| $E_{ij}$ (rydbergs) | 1.5595 | 1.6968 | 1.7450 |

[a] Analytic approximation to the DHM and WHE experimental data, eq. (9), with absolute values fixed by eq. (12).

[b] See Table 2 for this notation.

TABLE 4

EXPERIMENTAL He $^1S$–$n$ $^1P^o$ ELECTRON CROSS SECTIONS (DHM, WHE) SCALED AND FITTED TO AN ANALYTIC APPROXIMATION ($10^{-18}$ cm$^2$)[a]

| | $2\,^1P^o$ | | | $3\,^1P^o$ | | | $4\,^1P^o$ | |
|---|---|---|---|---|---|---|---|---|
| $E$ | Eq. (9)[a] | DHM[b] | WHE[c] | Eq. (9) | DHM | WHE | Eq. (9) | DHM |
| 22..... | 1.08 – 1[d] | ... | ... | ... | ... | ... | ... | ... |
| 23..... | 3.79 – 1 | ... | ... | ... | ... | ... | ... | ... |
| 24..... | 7.44 – 1 | ... | ... | ... | ... | ... | 1.460 – 2 | ... |
| 25..... | 1.165 | ... | ... | ... | ... | ... | 6.918 – 2 | ... |
| 30..... | 3.408 | 3.49 | 3.47 | 5.82 – 1 | 6.97 – 1 | 6.50 – 1 | 3.029 – 1 | 3.03 – 1 |
| 40..... | 6.659 | 6.48 | 5.96 | 1.400 | 1.32 | 1.21 | 6.143 – 1 | 6.06 – 1 |
| 50..... | 8.37 | 8.35 | 7.60 | 2.166 | 1.73 | 1.62 | 8.01 – 1 | 8.11 – 1 |
| 60..... | 9.24 | 9.26 | 8.83 | 2.097 | 2.03 | 1.90 | 9.16 – 1 | 9.38 – 1 |
| 70..... | 9.66 | 9.63 | 9.06 | 2.216 | 2.36 | 2.05 | 9.85 – 1 | 1.01 |
| 80..... | 9.81 | 9.82 | 9.41 | 2.265 | 2.48 | 2.13 | 1.024 | 1.04 |
| 85..... | 9.83 | 9.87 | ... | ... | ... | ... | ... | ... |
| 90..... | 9.82 | 9.84 | 9.41 | 2.274 | 2.52 | 2.15 | 1.042 | 1.05 |
| 100..... | 9.74 | 9.74 | 9.37 | 2.258 | 2.52 | 2.14 | 1.046 | 1.05 |
| 150..... | 8.78 | 8.78 | 8.51 | 2.041 | 2.33 | 1.98 | 9.67 – 1 | 9.7 – 1 |
| 200..... | 7.747 | 7.81 | 7.70 | 1.805 | 2.01 | 1.83 | 8.60 – 1 | 8.6 – 1 |
| 500..... | 4.579 | 4.63 | 4.70 | 1.086 | 1.15 | 1.13 | 4.998 – 1 | 5.1 – 1 |
| 1000..... | 2.903 | 2.88 | 2.91 | 6.906 – 1 | 7.06 – 1 | 6.96 – 1 | 3.039 – 1 | 3.1 – 1 |
| 2000..... | 1.747 | 1.73 | 1.72 | 4.169 – 1 | 4.17 – 1 | 4.11 – 1 | 1.805 – 1 | 1.9 – 1 |

[a] See eqs. (9) and (13), and Table 1.
[b] Normalized data from DHM.
[c] Normalized data from WHE
[d] See Table 2 for this notation.

where $T_e$ is electron temperature in units of $E_{ij}$, and $E_n(Y)$ is the exponential integral of order $n$. The rate coefficient for the excitation transition is then given by

$$k_{ij}(T_e) = (2\pi m)^{-3/2}\phi^{-1/2}h^2T_e^{-1/2} \times [\Omega_{ij}(Y)/\omega_i] \exp(-Y)\ \text{cm}^3\ \text{s}^{-1}, \quad (16)$$

where $m$ is electron mass, $\phi$ is the Boltzmann constant, and

$$(2\pi m)^{-3/2}\phi^{-1/2}h^2 = 8.629 \times 10^{-6}$$

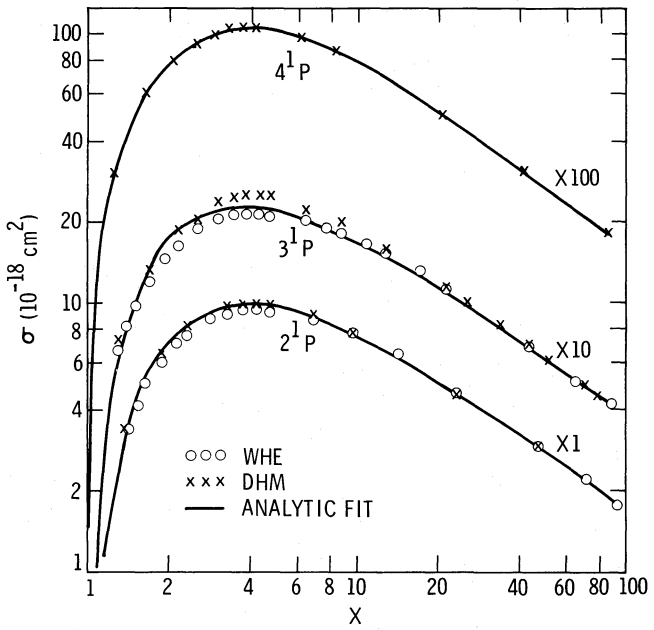


FIG. 7.—Analytic cross sections of the He 1 $^1S$–2 $^1P$, 3 $^1P$, 4 $^1P$ states plotted in dimensionless (threshold) energy units ($X$) against observational data (see Table 4). *Circles*: WHE; *crosses*: DHM; *solid curve*: analytic function (eqs. [6], [9], and [12]; Table 3).

if $T_e$ is in Kelvin. Aggarwal, Kingston, and McDowell (1984) also give rate coefficients for helium with a different formulation.

These results thus show compatibility well within experimental uncertainty of the He I $^1S$–$n$ $^1P^o$) series excitation cross sections with the Born approximation in the high-energy regime. The extrapolation of the coefficients for the He I $^1S$–$n$ $^1P^o$) transition in Table 3 to higher members of the series is difficult because of nonlinear trends in the $C_n$ ($n < 7$) coefficients. We recommend that the relative values of $C_n$ for the $^1S$–4 $^1P$ transition be applied to the higher orders, using equation (12) to establish absolute values, in order to provide cross sections with reasonable validity down to excitation threshold.

The excitation functions for ionization-excitation of He are distinctly different from the allowed neutral transitions. The experimental measurements of the cross section shapes for the 4$l$, 3$l$, and 2$p$ states of He II are all in good agreement. The derived shapes of the collision strengths plotted in threshold units ($X$) are sufficiently similar to allow the application of the same relative collision strength parameters in analytically fitting the excitation cross sections of all of the observed transitions. The collision strengths for the various experimental measurements of the He II transition are shown in Figure 6. along with theoretical data. For values $X \gtrsim 10$ the experimental collision strengths are very nearly constant, showing a distinct divergence from a first Born approximation curve. Fitting the excitation function shown in Figure 5 using equation (9) results in a small Born approximation constant ($C_7$) that could be set to zero within experimental error, and the dominant coefficient over the important energy range is $C_5$. A sufficiently accurate fit to the cross sections from threshold is obtained using six coefficients, $C_1 \ldots, C_5$ and $\alpha$ (eq. [9]). The Forand, Becker, and McConkey (1985) measurements of the 1$s$–2$p$ 30.4 nm transition are included in Figure 6 and, along with the data of Moustafa Moussa and de Heer (1967) and Bloemen *et al.* (1981), show basically the same energy dependence as that of the $n = 3$ and $n = 4$ states. On this basis the recommended

collision strengths for the excited states are given in Table 3 in terms of the coefficients of equation (9), so that excitation functions can be obtained analytically for any excitation energy. The theoretical calculations of Dalgarno and McDowell (1956) and Lee and Lin (1965) are also shown in Figure 6. The shapes of the theoretical collision strengths show a Born dipole allowed transition characteristic with increasing collision strengths for $X \gtrsim 3$, distinctly different from the experimental data. The collision strength for total ionization of He is shown in Figure 6 as measured by Rapp and Golden (quoted in Kieffer and Dunn 1966). Most of the ionization process obviously branches into the ground He II 1*s* state, and the excitation function is clearly quite different from those of the higher states because the 1*s* function has a strong first Born approximation component (Fig. 6, Table 3). The theoretical calculations of Dalgarno and McDowell (1956) for ionization of He into the He II 1*s* state does not fit the experimental work particularly well, either in magnitude (Table 3) or in shape (Fig. 6). The relative magnitudes of the constants for the 1*s* state are distinctly different from those of the excited states (Table 3). The excited states show a high-energy asymptote with $\sigma \propto 1/E$, whereas the 1*s* cross section shows $\sigma \propto 1/E \ln E$ Bethe-Born shape.

## IV. CONCLUSIONS

The cross sections for the He I $1s^2\ ^1S$–$1snp\ ^1P^o$ series have been measured using a relative flow method, with the absolute scale fixed by the H Ly$\alpha$ dissociative excitation cross section standard (Paper I). The cross sections can also be estimated using the Born approximation, and a comparison using an improved analytic method with the DHM and WHE experimental data yields values generally lower than the original (DHM, WHE) analysis based on Fano plots. The good agreement between the present absolute measurements of the He cross sections and the Born approximation can be taken as a measure of the accuracy of the H Ly$\alpha$ transfer standard and the estimated relative sensitivity of the spectrometer. The new method has been suggested as a more accurate means of converting measured relative excitation functions to an absolute scale through application of the Born approximation. The method does not require an extrapolation technique. However, both the new method and the Fano plot technique require accurate relative excitation function measurements extended to high energy.

Cross sections for the ionization-excitation of the He II 121.51 nm and He II 164.04 nm transitions have been measured. The results, together with earlier experimental work, strongly suggest that theoretical calculations of the reactions differ fundamentally from physical reality. The theoretical calculations by Lee and Lin (1965) and Dalgarno and McDowell (1956), which are now 20 years old or more, made use of Born theory in approximating the calculations of the cross section of the double electron excitation process. The failure of the theory to describe the experimental results stems from the neglect in the theory of electron correlation effects between the two orbital electrons. Physically, the dynamic repulsive interaction between the two orbital electrons was neglected in choosing unperturbed wave functions for the initial and final states. Today multiconfigurational representations of the ground state of helium exist but are not available for the final state. One modern approach to the theory could involve expansions in hyperspherical coordinates (Lin 1983; Peterkop 1977; Seaton 1983) for studying this optically forbidden process.

The authors wish to thank J. W. McConkey, S. Trajmar, and S. Federman for thorough reviews of the manuscript. We have also benefited from discussion with A. Dalgarno, B. Van Zyl, W. Westerveld, and J. Risley. This work was supported by the Air Force Office of Scientific Research (AFOSR) and by NASA Planetary Sciences and Astronomy/Relativity Programs, under contract NAS7-100 to the Jet Propulsion Laboratory, California Institute of Technology, Pasadena, CA 91109; NAGW-106 to the University of Southern California, Los Angeles, CA 90089; and NAGW-649 to the University of Arizona, Tucson, AZ 85717.

## REFERENCES

Aggarwal, K. M., Kingston, A. E., and McDowell, M. R. C. 1984, *Ap. J.*, **278**, 874.
Ajello, J. M. 1984, *Geophys. Res. Letters*, **11**, 1195.
Ajello, J. M., and Franklin, B. 1985, *J. Chem. Phys.*, **82**, 2519.
Ajello, J. M., and Shemansky, D. 1985, *J. Geophys. Res.*, in press.
Ajello, J. M., Shemansky, D. E., Yung, Y. L., and Kwok, D. 1984, *Phys. Rev. A*, **29**, 336.
Ajello, J. M., and Srivastava, S. K. 1981, *J. Chem. Phys.*, **75**, 4454.
Ajello, J. M., Srivastava, S. K., and Yung, Y. L. 1982, *Phys. Rev. A*, **25**, 2485.
Ayres, T. R., Linksy, J. T., Simon, T., Jordan, C., and Brown, A. 1983, *Ap. J.*, **274**, 784.
Bloemen, E. W. P., Winter, H., Mark, T. O., Dijkkamp, D., Barends, D., and de Heer, F. J. 1981, *J. Phys. B*, **14**, 717.
Clout, P. N., and Heddle, D. W. O. 1969, *J. Opt. Soc. Am.*, **59**, 715.
Dalgarno, A., and McDowell, M. R. C. 1956, in *The Airglow and the Aurorae*, ed. E. B. Armstrong and A. Dalgarno (New York: Pergamon), p. 340.
Donaldson, F. G., Hender, M. A., and McConkey, J. W. 1972, *J. Phys. B*, **5**, 1192 (DHM).
Fite, W. L., and Brackmann, R. T. 1958, *Phys. Rev.*, **112**, 1151.
Forand, L., Becker, K., and McConkey, J. W. 1985, *J. Phys. B*, in press.
Heddle, D. W. O., and Keesing, R. G. W. 1968, in *Advances in Atomic and Molecular Physics* (New York: Academic), p. 267.
Henry, R. J. W. 1981, *Phys. Rept. (Netherlands)*, **68**, 1.
Kieffer, L. J., and Dunn, G. H. 1966, *Rev. Mod. Phys.*, **38**, 1.
Kim, Y.-K., and Inokuti, M. 1968, *Phys. Rev.*, **175**, 176.
Lee, E. T. P., and Lin, C. C. 1965, *Phys. Rev. A*, **138**, 301.
Lin, C. D. 1983, *Phys. Rev. Letters*, **51**, 1348.
Malcolm, I. C., Dassen, H. W., and McConkey, J. W. 1979, *J. Phys. B*, **12**, 1003.
McFarlane, S. C. 1974, *J. Phys. B*, **7**, 1756.
Moustafa Moussa, H. R., and de Heer, F. J. 1967, *Physica*, **36**, 646.
Moustafa Moussa, H. R., de Heer, F. J., and Schutten, J. 1969, *Physica*, **40**, 5177.
Mumma, M. J., Misakian, M., Jackson, W. M., and Faris, J. L. 1974, *Phys. Rev. A*, **9**, 203.
Percival, I. C., and Seaton, M. J. 1958, *Phil. Trans. A*, **251**, 113.
Peterkop, R. K. 1977, *Theory of Ionization of Atoms by Electron Impact*, ed. D. Hummer (Boulder: Colorado Associated University Press).
St. John, R. M., and Lin, C. C. 1964, *J. Chem. Phys.*, **41**, 195.
Seaton, M. J. 1962, in *Atomic and Molecular Processes* (New York: Academic), chap. 11.
———. 1983, *Rept. Progr. Phys.*, **46**, 167.
Shemansky, D. E., and Ajello, J. M. 1983, *J. Geophys. Res.*, **88**, 459.
Shemansky, D. E., Ajello, J. M., and Hall, D. T. 1985, *Ap. J.*, **296**, 765 (Paper I).
Shull, J. M. 1979, *Ap. J.*, **234**, 761.
Srivastava, S. K., Chutjian, A., and Trajmar, S. 1975, *J. Chem. Phys.*, **63**, 2659.
Trajmar, S., and Register, D. 1984, in *Electron Molecule Collisions*, ed. K. Takayanagi and I. Shimamura (New York: Plenum), chap. 6.
Van Eck, J., and de Jongh, J. P. 1970, *Physica*, **47**, 141.
Westerveld, W. G., Heideman, H. G. M., and Van Eck, J. 1979, *J. Phys. B*, **12**, 115 (WHE).
Wiese, W. L., Smith, C. W., and Glennon, B. M. 1966, *Atomic Transition Probabilities*, Vol. **1** (NSRDS–NBS 4).

J. M. AJELLO and B. FRANKLIN: Mail Stop 183-601, Jet Propulsion Laboratory, 4800 Oak Grove Drive, Pasadena, CA 91109

D. T. HALL and D. E. SHEMANSKY: Lunar and Planetary Laboratory, University of Arizona, 3625 E. Ajo Way, Tucson, AZ 85713